

## Short Note

# The accuracy of wave-equation migration amplitudes

*Douglas Gratwick*<sup>1</sup>

## INTRODUCTION

When migrating seismic data for the purpose of reservoir characterization, it is necessary to use a migration algorithm that preserves relative amplitude trends (Scheriff, 1995). In the industry, this is usually attained using Kirchhoff methods with asymptotic Green's functions (Biondi, 2000). This method is useful in many geologic settings, but when a complex velocity Earth introduces more complex wave propagation phenomena, “wave-equation” migration (WEM) based on downward continuation becomes more attractive (Prucha et al., 1999).

The goal of this paper is to address the problems associated with amplitude preservation encountered in WEM and how to correct them, at least to first order. Three effects will be discussed:

1. The “squeeze” effect, where  $P_h$  coverage is reduced.
2. The “under-migrated” amplitude effect, where a hypothetical constant amplitude reflector shows decreasing amplitude magnitude at larger  $P_h$ .
3. The “over-migrated” amplitude effect, where the opposite occurs, and amplitudes increase with larger  $P_h$ .

This paper shows that for relatively simple velocity models, a weight described by Sava and Biondi (2001) perfectly preserves amplitude trends. Also we outline a method to mute parts of an image gather outside the coverage of the recording geometry.

## MIGRATION ALGORITHM

The migration algorithm used is a variation of the split-step method (Stoffa et al., 1990). A brief description of the basic algorithm can be found in this report (Gratwick, 2001). Our

---

<sup>1</sup>email: doug@sep.stanford.edu

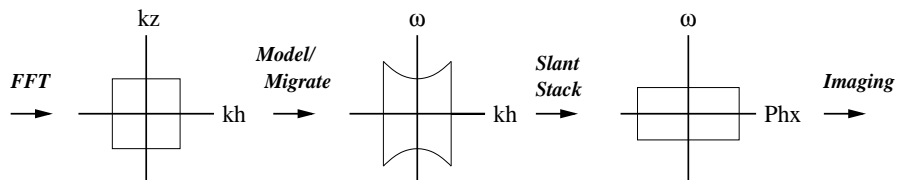
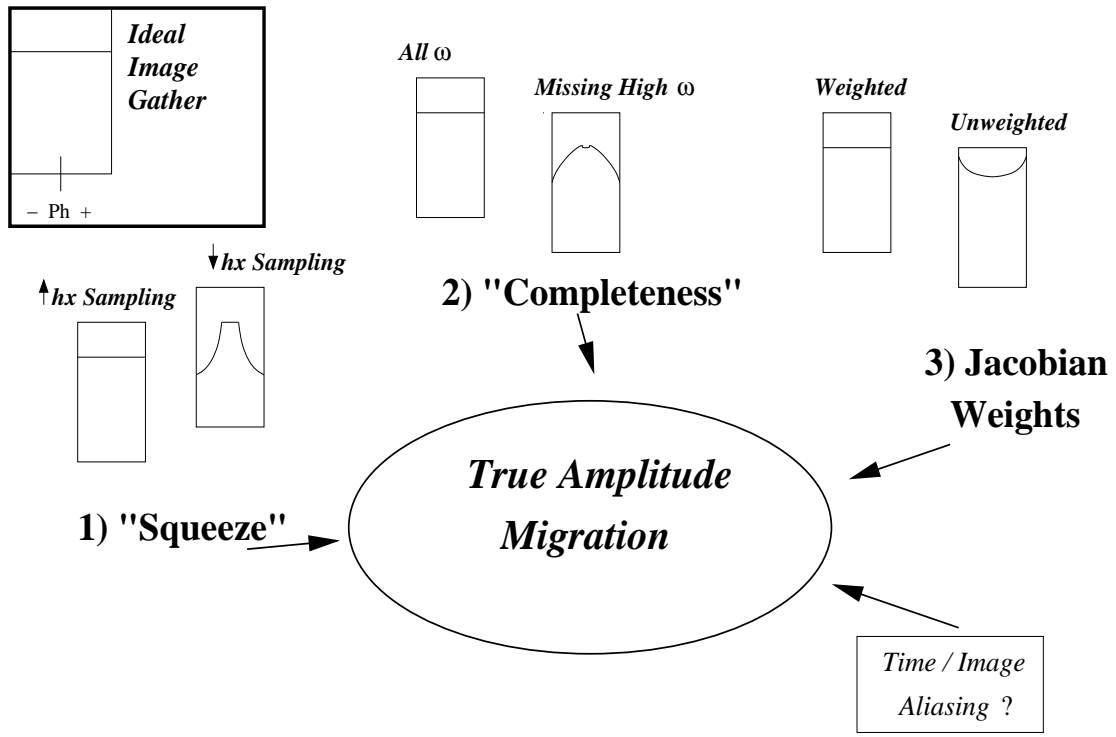


Figure 1: Factors affecting amplitudes. The modeling/migration workflow is shown below.  
 doug2-flow [NR]

image gathers are a function of offset ray parameter,  $P_h$ , which is given by equation (1):

$$P_h = \frac{2 \sin \theta \cos \phi}{V(z, \mathbf{m})}, \quad (1)$$

where  $\theta$  is the incidence angle,  $\phi$  is the geologic dip, and  $V(z, \mathbf{m})$  is the local interval velocity function as a function of midpoint. The flow of the migration and the factors which affect amplitude preservation are outlined in Figure 1. All schematic image gathers are from a hypothetically flat, constant amplitude reflector. The expected image gather after true amplitude migration is seen in the upper-left corner of Figure 1.

## CORRECTION FOR CONSTANT AMPLITUDE

### “Squeeze” effect

The first effect to address is the “squeeze,” where  $P_h$  coverage is reduced, especially at higher frequencies. This is mainly a function of CMP trace sampling. Specifically, it is a function of half-offset wavenumber and frequency.  $P_h$  can be calculated by a radial trace transform in  $(\omega, k_h)$  domain using equation (2):

$$P_h = \frac{k_h}{\omega}, \quad (2)$$

where the maximum  $k_h$  is given as  $\frac{1}{2\Delta h}$ . So if we, sample twice as much in half-offset, the maximum  $k_h$  doubles, and our maximum  $P_h$  increases, as seen in Figure 2.

### “Under-migrated” effect

The second problem which can arise involves the completeness of our migration with respect to frequency. The range of  $\omega$  needed to cycle through is a function the data spectrum. Figure 3 shows a CMP gather in  $(\omega, k_h)$  domain. To be correct, our migration must cycle through the top and bottom lines in the plot. However, we must be careful not to cycle too high, as temporal aliasing is still a factor (maximum frequency can be no higher than the Nyquist,  $\frac{1}{2\Delta t}$ ).

### “Over-migrated” effect

The last problem is solved by applying the Jacobian weights discussed by Sava and Biondi (2001). Figure 4 shows what happens to our migrated amplitudes without using the proper weights. The top-left corner is the spectrum plot seen in Figure 3, with the lines at the top and bottom edges of the plot showing that we have now migrated up to 45 Hz. The bottom-left is our expected amplitude, and the top-right is a migrated image gather. Notice in the bottom-right, which is a graph of amplitude taken at 2 km depth, that amplitudes are actually increasing with increasing  $P_h$ . Obviously this will present a problem when trying to interpret AVA. With the weights applied, we see that the amplitude is much closer to constant (Figure 5).

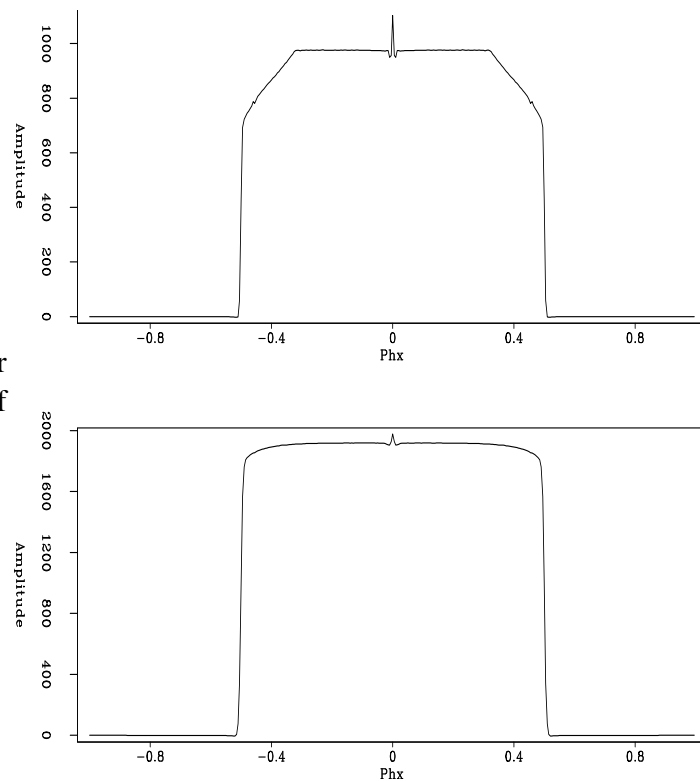


Figure 2: Two amplitude plots after migration. Bottom has half the  $\Delta h$  of the top. **doug2-kh\_compare** [CR]

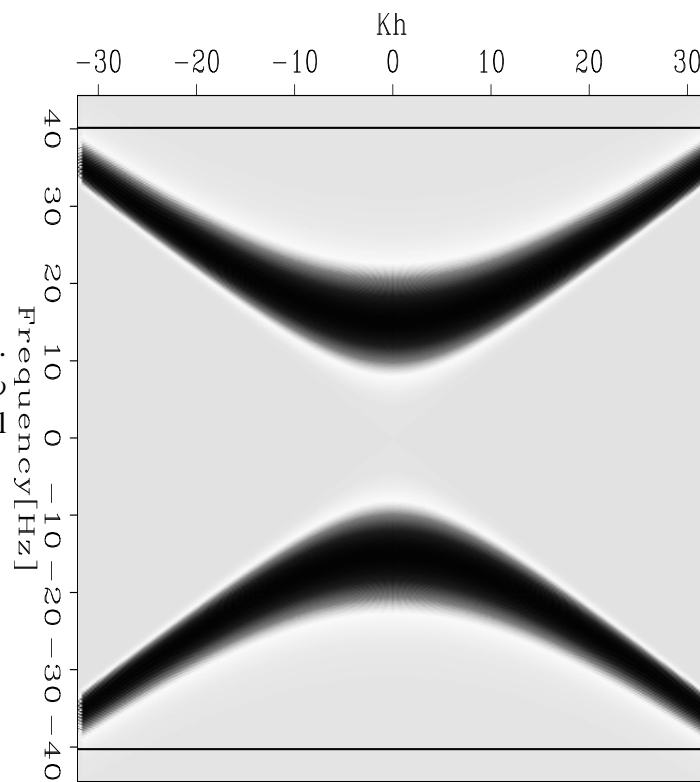


Figure 3: A CMP in  $(\omega, k_h)$  domain. We must cycle equal to or past  $\omega$  at the line, but not past temporal Nyquist. **doug2-spect** [ER]

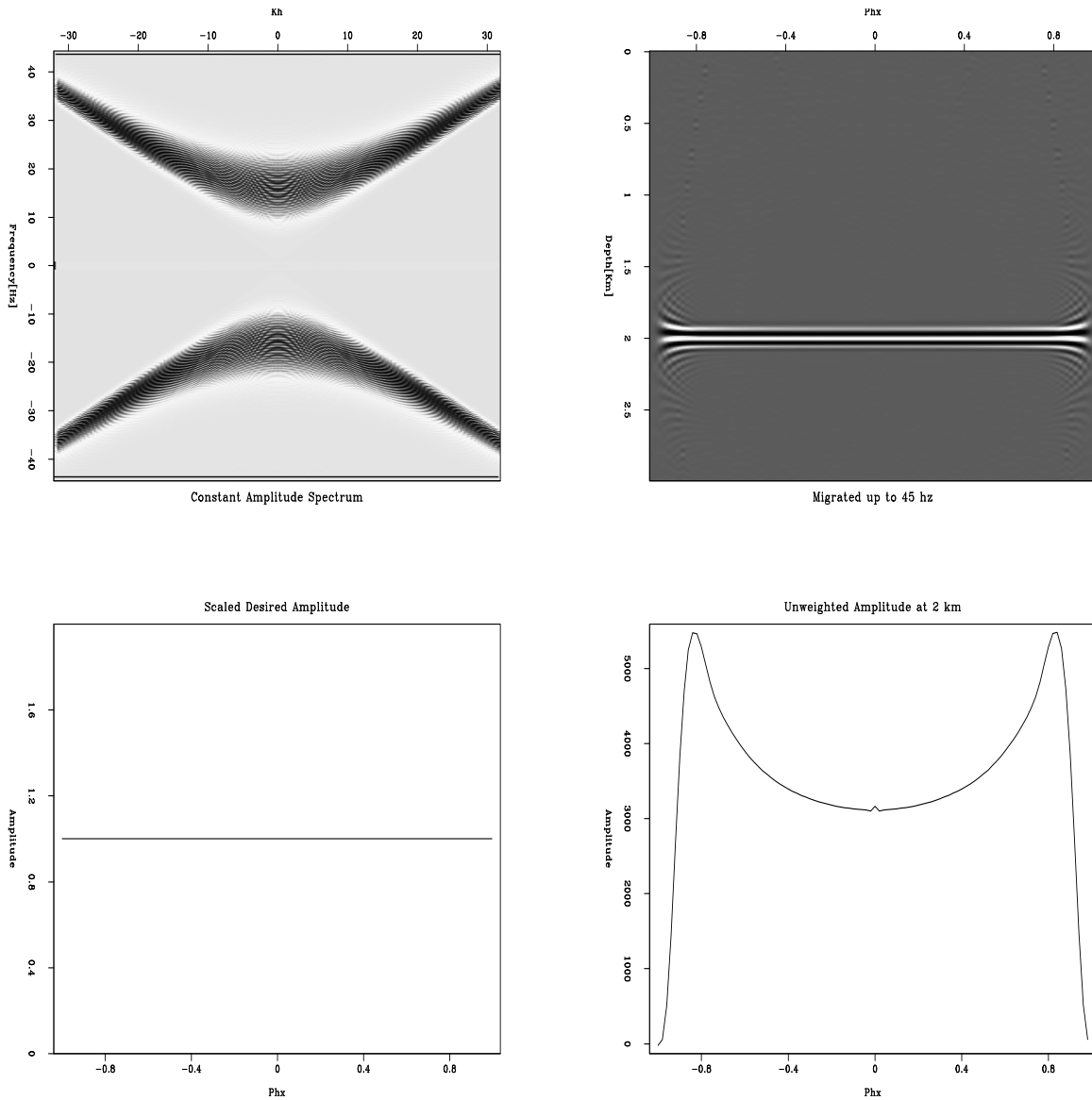


Figure 4: Unweighted migration to 45 Hz. Top left is the data spectrum, top right is the migrated image gather. Bottom left is the desired amplitude, and bottom right is the actual amplitude at 2 km. doug2-frame\_const\_45 [ER]

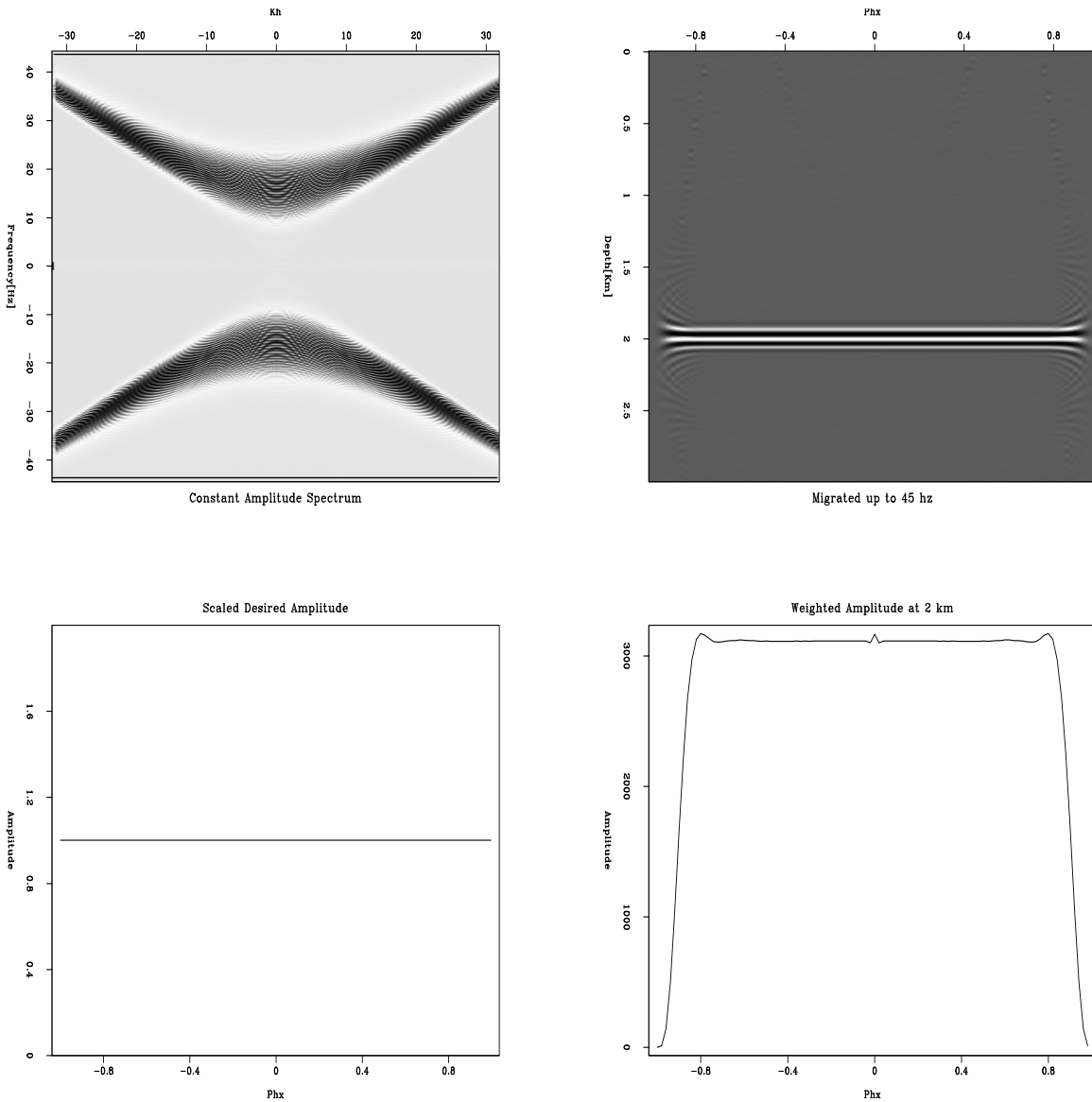


Figure 5: Weighted migration to 45 Hz. Top left is the data spectrum, top right is the migrated image gather. Bottom left is the desired amplitude, and bottom right is the actual amplitude at 2 km. doug2-frame\_constw\_45 [ER]

## CORRECTION FOR SYNTHETIC AMPLITUDE VARIATION WITH ANGLE

Our objective behind true amplitude migration is to use image gathers for amplitude variation with angle (AVA) analysis. We now present a case where the AVO intercept is positive, and there is a negative AVO gradient which causes a polarity reversal. This Class I AVO effect occurs in high impedance gas sands, present in continental environments, or in extremely deep water. The polarity reversal causes the classic “dim spot” in stacked sections (Rutherford and Williams, 1989). Figure 6 shows the same four panels as in Figures 4 and 5. The AVO gradient actually seems a little steeper in the migrated graph, however this is simply because the graph is normalized to zero, since energy drops to zero outside the maximum aperture of the migration. So in fact, the amplitude gradient is preserved perfectly.

## COMMON IMAGE GATHER APERTURE MUTE

Recording geometries limit the maximum offset ray parameter. However, our migration can put energy in part of the image gathers beyond this maximum aperture. Therefore a mute needs to be applied to this part of the image gathers. The maximum  $P_h$  is a function of the coefficients on the right side of equation (1) and is given by equation (3):

$$P_h(\max) = \frac{2 \tan^{-1}(\frac{h_{\max}}{z}) \cos \phi_{\max}}{V(z, \mathbf{m})}, \quad (3)$$

where  $h_{\max}$  is the maximum half offset,  $\phi_{\max}$  is the maximum expected geologic dip,  $z$  is depth, and  $V(z, \mathbf{m})$  is the midpoint interval velocity function. This simple relation is a reasonable approximation, but to truly define the migration aperture, ray-tracing needs to be used to account for the wavefield path above the reflector. Figure 7 shows identical image gathers, with the right panel having the mute applied. As expected, the deeper reflectors have a reduced maximum  $P_h$ .

The main use of this mute is to zero points outside of the migration aperture so that they are not used in our least-squares fit to find AVO intercept and AVO gradient (Gratwick, 2001).

## CONCLUSIONS

Since the tests presented in this paper are for constant velocity, we can assume that the Jacobian weights are correct to the first order. The use of these weights is necessary to do true amplitude migration. When doing true amplitude migration, we also must keep in mind spatial and temporal sampling to reduce “squeezing” and aliasing effects. Also, the use of an offset ray parameter mute is necessary so that points outside of the maximum migration aperture are not used in our AVA analysis.

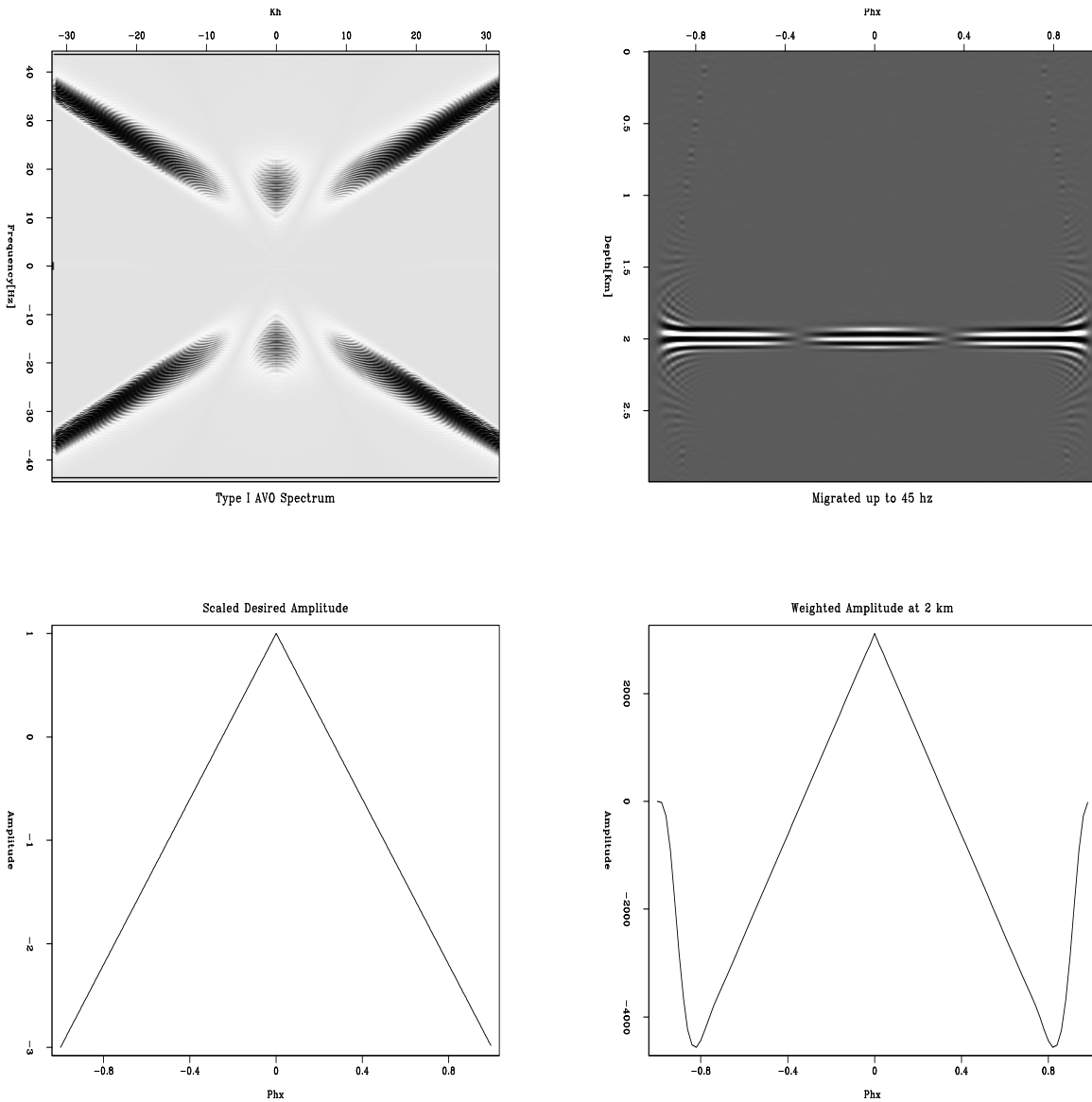


Figure 6: Weighted migration to 45 Hz. Top left is the data spectrum, top right is the migrated image gather. Bottom left is the desired amplitude, and bottom right is the actual amplitude at 2 km. doug2-frame\_t1w\_45 [ER]

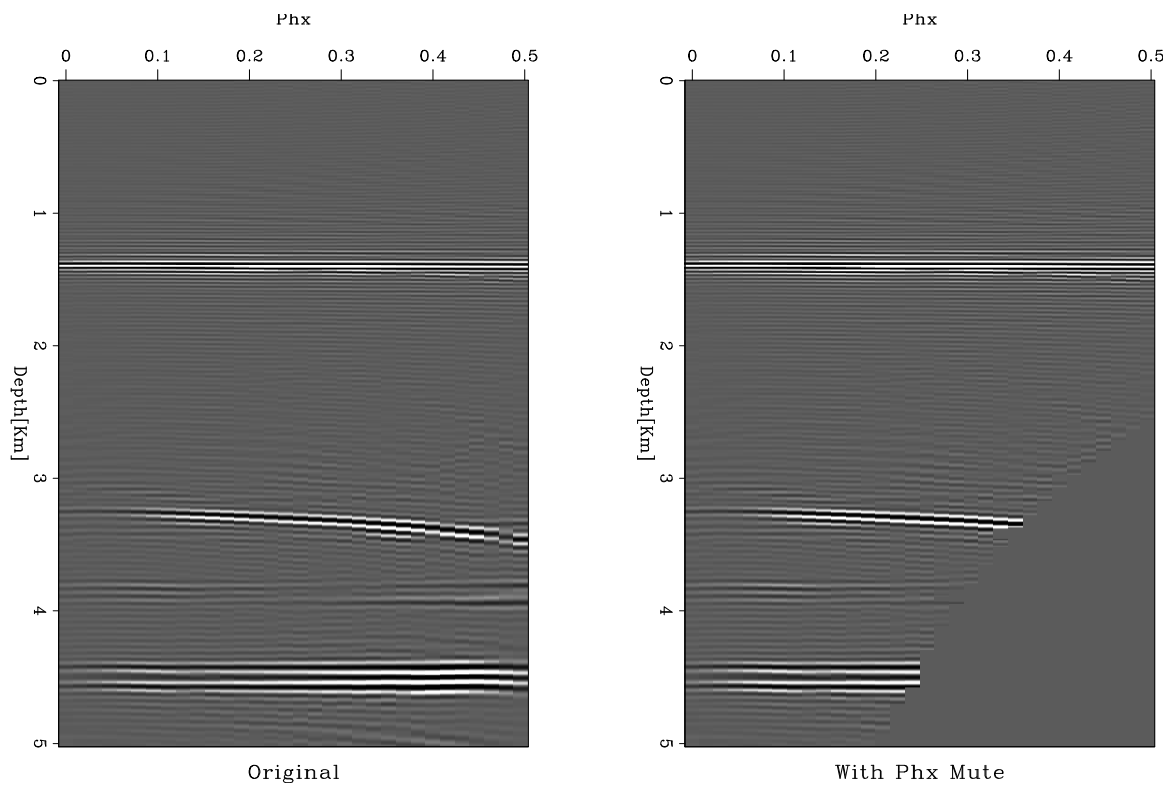


Figure 7: Identical image gathers. Right shows the result of the  $P_h$  mute. `doug2-ph_mute` [ER]

**REFERENCES**

Biondi, B., 2000, 3-D Seismic Imaging: Class notes,  
<http://sepwww.stanford.edu/sep/prof/index.html>.

Gratwick, D., 2001, Amplitude analysis in the angle domain: **SEP-108**, 45–62.

Prucha, M., Biondi, B., and Symes, W., 1999, Angle-domain common image gathers by wave equation migration: 69th Ann. Internat. Meeting, Soc. Expl. Geophysicists, Expanded Abstracts, **1**, 824–827.

Rutherford, S. R., and Williams, R. H., 1989, Amplitude-versus-offset variations in gas sands: *Geophysics*, **54**, no. 6, 680–688.

Sava, P., and Biondi, B., 2001, Amplitude-preserved wave-equation migration: **SEP-108**, 1–26.

Scheriff, R., 1995, *Exploration Seismology*: Cambridge.

Stoffa, P. L., Fokkema, J. T., de Luna Freire, R. M., and Kessinger, W. P., 1990, Split-step Fourier migration: *Geophysics*, **55**, no. 4, 410–421.